

# Feature points tracking by using photometric model and colorimetric invariants

M. Gouiffès<sup>(1)</sup> C. Collewet<sup>(2)</sup> C. Fernandez-Maloigne<sup>(1)</sup> A. Trémeau<sup>(3)</sup>

<sup>1</sup> Laboratory SIC, University of Poitiers

<sup>2</sup> INRIA/IRISA Rennes, France

<sup>3</sup> Laboratory LIGIV EA 3070, University Jean Monnet, France

SIC, Bd Marie et Pierre Curie, Téléport 2  
BP 30179  
86962 Futuroscope, Chasseneuil Cedex  
France

gouiffes@sic.sp2mi.univ-poitiers.fr

## Abstract

*This article proposes several colour points tracking methods which are robust to illumination changes. Firstly, the illumination correction is achieved by computing simultaneously a local photometric model and a motion model during the image sequence. Secondly, some colour invariants are used to compensate in each point for the illumination changes. Then, since most of these attributes are not sufficiently robust to model specular highlights occurrence, we propose a third method which jointly uses a local photometric model and a global correction, by using colour invariants. To finish, the three methods are compared through experimental results, on images sequences where specular highlights and lighting changes appear.*

## Introduction

Many computer vision algorithms rely on the accurate and robust matching of features between several frames through an image sequence, for example 3D reconstruction, video surveillance or visual servoing. The feature points have proved to be the only available feature in non-structured scenes, where no edges or lines can be extracted, such as in agricultural, spatial, medical or underwater applications [1]. In addition, the whole of the points are not likely to be occluded at the same time. Nevertheless, using points is difficult since the only information available is the luminance (or the colour) of the neighboring pixels around the points to be tracked. In the seminal approaches, the luminance (or the colour) was assumed to be constant between successive frames, as in [9, 13] for luminance images, or [7] for colour. Although some more robust approaches have been proposed thereafter, all of them are based on those same photometric constraints. These methods assume that the objects are lambertian and that no lighting changes occur during the whole sequence. However, in order to cope with bias and gain changes, a photometric normalization can be achieved [14]. In a similar manner, Jin *et al.* [8] have proposed to compensate for an affine photometric model in luminance images. In this work, the bias and the gain are estimated during the image sequence in order to improve the computation of the motion model.

Few works about colour points tracking have to be related. However, because of the additional information provided by the colour image, a larger number of points can be selected and tra-

cked in colour image sequences. Although two points have the same luminance, they can have different colours.

In this article, we propose several solutions to improve the robustness of points tracking according to specular highlights and illumination changes, by using colour attributes. Firstly, in the next section, we study the modeling of colour changes occurring during an image sequence. Secondly, the third section focuses on the use of colour invariants. The most efficient invariants do not compensate sufficiently well for specular highlights. Nevertheless, we improve the tracking process by jointly computing the colour invariants (which compensates for lighting changes) with the photometric model (which models the illumination changes). The fourth section will study the use of the photometric model and invariants in the tracking process.

These different techniques will be compared by considering several image sequences, which show some specular highlights variations and lighting changes.

## Modeling of colour changes

The observed colour of a surface depends on several parameters such as the scene geometry (lighting, camera and objects locations) and the surface properties (roughness, reflectance). This physical phenomenon can be expressed by the use of reflection models, which are largely used in computer graphics, such as the Phong model [11] and the Torrance-Sparrow one [15]. We consider a camera which moves and acquires an image sequence of a scene. The latter can also be in motion. We will call  $\mathbf{f}$  and  $\mathbf{f}'$  the colour images acquired respectively at time  $k$  and  $k'$ . Figure 1 shows the geometry of the scene which is used in the explanation of the photometric changes.

### Colour model

Let be a point  $P$  of the object projected in  $\mathbf{f}$  at point  $p$  of coordinates  $(x_p, y_p)$ . Owing to most reflection models [11, 15], the colour in  $p$  can be expressed by :

$$\mathbf{f}(p) = \mathbf{C}_d(p) \cdot \mathbf{a}(p)m_d(p) + \mathbf{C}_s(p)h_f(p) + \mathbf{C}_a \quad (1)$$

where  $\mathbf{a}$  is related to the *albedo* and depends on the reflectance of the surface,  $\mathbf{C}_s$  is the colour of specular component,  $\mathbf{C}_d$  the colour of direct light and  $\mathbf{C}_a$  is the colour of the ambient light. Let us notice that «  $\cdot$  » represents the Hadamard product.  $h_f$

expresses the specular function in image  $\mathbf{f}$  and refers to the scene geometry and to the surface properties. For example, with Torrance-Sparrow model [15], we have :

$$m_d(p) = \cos \theta_i(P) \text{ and } h_f(p) = \exp\left(\frac{-\rho(P)^2}{2\zeta^2}\right) / \cos \theta_r(P) \quad (2)$$

where  $\theta_i$  is the angle between the normal  $\mathbf{n}$  in  $P$  and the lighting direction  $\mathbf{L}$ .  $\rho$  is the angle between  $\mathbf{n}$  and the bisecting line between the viewing and the lighting vectors  $\mathbf{V}$  and  $\mathbf{L}$ .  $\zeta$  expresses the roughness of the material. Thus, the specular component  $h_f$  reaches its maximum value when  $\rho = 0$ . On the other hand, the higher  $\zeta$  is, the more quickly  $h_f$  will vary in the image.

By using this colour model, we can deduce an analytic expression of colour changes between two frames.

### Colour changes

Let us consider that a second image  $\mathbf{f}'$  is acquired after a relative motion between the scene and the camera. Then, point  $P$  is projected in  $p'$  in image  $\mathbf{f}'$ . Furthermore, an illumination change can occur between  $\mathbf{f}$  and  $\mathbf{f}'$ . Consequently, the colour  $\mathbf{f}'(p')$  at time  $k'$  can be expressed as a function of  $\mathbf{f}$  at time  $k$  as follows :

$$\mathbf{f}'(p) = \mathbf{f}(p) + \boldsymbol{\Psi}(p) \quad (3)$$

In case of specular highlights variations, only  $h_f(p)$  varies in equation (1) and we show that  $\boldsymbol{\Psi} = \boldsymbol{\Psi}_1(p)$  with the following definition of  $\boldsymbol{\Psi}_1(p)$  [4] :

$$\boldsymbol{\Psi}_1(p) = \mathbf{C}_s(p)(h_{f'}(p) - h_f(p)) \quad (4)$$

where  $h_{f'}(p)$  is the specular reflection component in image  $\mathbf{f}'$ . In case of both lighting changes and specular highlights occurrence  $\boldsymbol{\Psi} = \boldsymbol{\Psi}_2(p)$  [4] :

$$\boldsymbol{\Psi}_2(p) = \mathbf{t}_d(p) \cdot \mathbf{a}(p)[\cos \theta_i(P) \cos t_i(P) - \sin \theta_i(P) \sin t_i(P)] + \mathbf{t}_s(p)h_g(P) + \boldsymbol{\Psi}_1(p) + \mathbf{t}_a(p) \quad (5)$$

where  $t_i$ ,  $\mathbf{t}_d$  and  $\mathbf{t}_a$  refer respectively to the changes of lighting angle  $\theta_i$ , of direct lighting colour  $\mathbf{C}_d$  and ambient light colour  $\mathbf{C}_a$ .

The expressions (4) and (5) use a large number of parameters which are not easily computable without any knowledge about the properties of the materials or the geometry of the scene. Consequently, their use is difficult in computer vision applications. However, some simple local approximations are often used : in indexing [5], tracking [8] or optical flow [10] contexts for example. The validity of such photometric models has been studied in [4]. In the following section, we describe the photometric model which is used in this article.

### Local approximation of colour changes

Let be  $\mathcal{W}$  a small window of interest centered on the point to be tracked  $p$ . In computer vision, most local photometric models defined on  $\mathcal{W}$  only assume a change of bias and/or gain of the camera (the affine model proposed by [8] for example). Under this assumption, the two parameters of the model are constant at each pixel of the window  $\mathcal{W}$ . However, according to (4) and (5),  $\boldsymbol{\Psi}$  is not a constant function since it depends on the vectors  $\mathbf{n}$ ,  $\mathbf{V}$ ,  $\mathbf{L}$ , which can be different at each point of  $\mathcal{W}$ , especially when the surface projected on  $\mathcal{W}$  is non-planar.

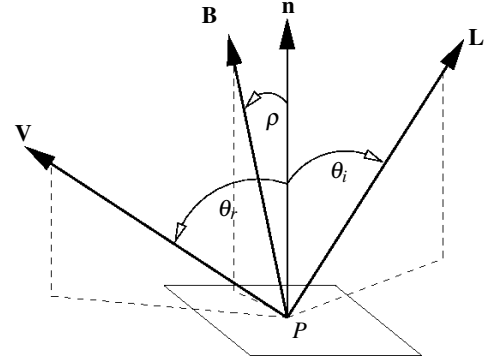


FIG. 1. Vectors and angles involved in the reflection description.

We assume that the function  $\boldsymbol{\Psi}$  can be correctly approximated by a continuous function in each point  $q$ , of coordinates  $(x, y)$ , located in the window  $\mathcal{W}$ . Thereby, this approximation can be expanded in Taylor series around the point to be tracked  $p$ . By neglecting the highest orders, we obtain the following photometric model :

$$\mathbf{f}'(q) \simeq \mathbf{f}(q) + \boldsymbol{\alpha}(x - x_p) + \boldsymbol{\beta}(y - y_p) + \boldsymbol{\gamma} \quad (6)$$

where  $\boldsymbol{\gamma} = \mathbf{f}(p)$  and  $\boldsymbol{\alpha}$ ,  $\boldsymbol{\beta}$  are the partial derivatives of  $\mathbf{f}$  in directions  $x$  and  $y$  respectively. The model (6) is particularly well adapted for specular highlights occurrence, which is not correctly modeled by using an affine photometric model (bias and gain). It is valid locally, for surfaces which do not have any coarse discontinuity of curvature or roughness in  $\mathcal{W}$ . Indeed, according to (4) and the expression of  $h_f$  given by (2),  $\boldsymbol{\Psi}_1$  depends on the angles and on the roughness, which are supposed to vary smoothly in  $\mathcal{W}$ .

The main limitation of this model appears when lighting changes occur as in (5), since the reflectance  $\mathbf{a}$  has to vary smoothly in  $\mathcal{W}$ , which is not true in general. Yet, the model (6) is available on small windows of interest, such as the windows that are used in the context of feature points tracking. The following section exposes a second way to cope with illumination changes, by using colour invariants.

### Invariant attributes

Most colour invariants are based on the dichromatic model [12], which is equivalent to (1) when  $\mathbf{C}_a = 0$ . It supposes a single light source, no ambient lighting and no interreflection. Most invariants imply that the illuminant is white :  $\mathbf{C}_s = \mathbf{C}_d = I(p)$ . Therefore, only the illuminant intensity  $I(p)$  (and not its colour) is supposed to vary. They also assume that a white balance has been achieved so that the integrals of each sensor sensibility over the wavelengths are the same on each sensor. We call  $Q$  this value. Consequently, the model (1) becomes :

$$\mathbf{f}(p) = I(p)\mathbf{a}(p)m_d(p) + I(p)h_f(p)Q \quad (7)$$

Note that  $\mathbf{a}(p)$  only depends on reflectance and sensor properties, which are supposed to be constant during the sequence. We distinguish two classes of colour invariants, which are related to lambertian or specular surfaces :

- *Lambertian surfaces.* In that case, the term  $I(p)Q(p)h_f(p)$  vanishes in (7). Thus, a ratio of two colour components cancels  $I(p)$  and  $m_d(p)$  and depends only on the constant parameters  $\mathbf{a}(p)$ . In this article, we use  $L_1$  and  $L_2$  norms and  $c_1c_2c_3$  invariants [2].

• *Specular surfaces.* According to (7), the difference of two colour components cancels the specular term  $I(p)Q(p)h_f(p)$ . Then, the ratio of two differences cancels  $I(p)$  and  $m_d(p)$ . We use the following invariant  $a_1 a_2 a_3$  :

$$a_1 = \frac{R-G}{D_a}, a_2 = \frac{R-B}{D_a} \text{ and } a_3 = \frac{G-B}{D_a}$$

with  $D_a = |R-G| + |G-B| + |B-R|$ .

Unfortunately, colour invariants are undefined or are very noisy for low intensities ( $L_1$  and  $L_2$  norms,  $c_1 c_2 c_3$ ) and/or low saturation ( $a_1 a_2 a_3$ ).

$L_1$ ,  $L_2$  and  $c_1 c_2 c_3$  do not make up for specular highlights but compensate well for lighting variations. By considering the  $L_1$  values, we can express the part of illumination changes which is not compensated by the invariant attributes so that

$$\mathbf{f}'_{L_1}(p) = \mathbf{f}_{L_1} + \boldsymbol{\Psi}_{L_1} \quad (8)$$

where  $\boldsymbol{\Psi}_{L_1}$  can be described with respect to the scene geometry and the material properties. Let be  $K_1(p) = I(p)m_b(p)$  and  $K_2 = I(p)h_f(p)Q$ . Then :

$$\boldsymbol{\Psi}_{L_1} = \frac{K_2(p)(a_G(p) + a_B(p) - 2a_R(p))}{K_1(p)\Sigma^2 + 3K_2(p)\Sigma} \quad (9)$$

with  $\Sigma = (a_R(p) + a_G(p) + a_B(p))$ . We assume that these residuals can be correctly approximated on a small window  $\mathcal{W}$  by a continuous function. The latter can be estimated by a Taylor series around the point to be tracked  $p$  :

$$\mathbf{f}'_{L_1}(q) \approx \mathbf{f}_{L_1} + \boldsymbol{\alpha}_{L_1}(x - x_p) + \boldsymbol{\beta}_{L_1}(y - y_p) + \boldsymbol{\gamma}_{L_1}. \quad (10)$$

When the illuminant is white  $\boldsymbol{\alpha}_{L_1}$ ,  $\boldsymbol{\beta}_{L_1}$  and  $\boldsymbol{\gamma}_{L_1}$  are scalar values. Nevertheless, the use of vectors can compensate for colour variations of the specular reflection component. Consequently, the white illuminant constraint is less restricting. The next section explains the use of the photometric model and the colour invariants in the context of feature points tracking.

## Tracking methods

The first tracking method consists in computing the motion model  $\delta(q, \boldsymbol{\mu})$ , parametrized by  $\boldsymbol{\mu}$  of a small window of interest  $\mathcal{W}$  centered on  $p$  by minimizing the following relationship [9, 13, 7] :

$$\varepsilon_1(\boldsymbol{\mu}) = \sum_{q \in \mathcal{W}} \|\mathbf{f}(q) - \mathbf{f}'(\delta(q, \boldsymbol{\mu}))\|^2 \quad (11)$$

$\mathbf{f}$  and  $\mathbf{f}'$  can be any vectorial images. In this article, we consider the colour invariants described in previous section :  $L_1$  and  $L_2$  norms,  $c_1 c_2 c_3$  and  $a_1 a_2 a_3$  attributes. Indeed, they show a good adequacy between invariance with respect to illumination changes and discrimination between colours. These methods will be compared with the use of luminance and  $RGB$  components.

In addition, we propose a second technique which takes the models (6) or (10) into account :

$$\varepsilon_2(\boldsymbol{\mu}) = \sum_{q \in \mathcal{W}} \|\mathbf{f}(q) - \mathbf{f}'(\delta(q, \boldsymbol{\mu})) + \mathbf{B}\mathbf{U}\|^2 \quad (12)$$

with  $\mathbf{U} = (x - x_p, y - y_p, 1)^T$ .  $\mathbf{B}$  is the matrix of the photometric parameters  $\mathbf{B} = (\boldsymbol{\alpha}, \boldsymbol{\beta}, \boldsymbol{\gamma})$ . Let be  $\mathbf{D} = [\boldsymbol{\mu}^T, \mathbf{B}^T]^T$ . In this paper, we compute an affine motion model between the initial frame  $\mathbf{f}$

and the current one  $\mathbf{f}'$ . Consequently, we assume a little variation  $\mathbf{d}$  around an estimate  $\hat{\mathbf{D}}$ ,  $\mathbf{D} = \hat{\mathbf{D}} + \mathbf{d}$ , so that (12) can be linearized in  $\mathbf{d}$ . Consequently, the method consists in solving the following linear system

$$\left( \sum_{m \in \mathcal{W}} \mathbf{V}_p \mathbf{V}_p^T \right) \mathbf{d} = \frac{1}{3} \sum_{m \in \mathcal{W}} \left( \sum_i (f_i(q) - f'_i(\delta(q, \hat{\boldsymbol{\mu}}) - \mathbf{U}^T \mathbf{B}_i) \mathbf{V}_p^i) \right) \quad (13)$$

where  $\mathbf{B}_i = (\alpha_i, \beta_i, \gamma_i)^T$  where  $i$  is one of the components ( $RGB$  or colour invariants). The vector  $\mathbf{V}_p^i$  and  $\mathbf{V}_p$  are expressed :

$$\mathbf{V}_{P_i} = \left[ f'_x{}^i, f'_y{}^i, x f'_x{}^i, x f'_y{}^i, y f'_x{}^i, y f'_y{}^i, x - x_p, y - y_p, 1 \right]^T \quad (14)$$

$$\mathbf{V}_P = \left[ f'_x, f'_y, x f'_x, x f'_y, y f'_x, y f'_y, x - x_p, y - y_p, 1 \right]^T \quad (15)$$

where  $f'_x$  and  $f'_y$  refer to the sum of the derivatives of the three colour components of  $\mathbf{f}'$  according to  $x$  and  $y$ . Let us notice that the matrix used to compute  $\mathbf{d}$  is not well-conditioned and requires a pre-conditioning.

These tracking methods will be compared in the following section.

## Experiments

Several experiments are carried out on sequences where specular highlights and/or lighting changes occur. In order to compare the tracking techniques, the points selected in the initial frame must be the same for each method, although the colour attributes are different.

### Detecting points

The points detection in luminance images [6] has been extended to colour [3]. It consists in computing the matrix  $M(p)$  at each pixel  $p$  of the initial image :

$$M(p) = \begin{pmatrix} \sum_{\mathcal{W}} (R_x^2 + G_x^2 + B_x^2) & \sum_{\mathcal{W}} (R_x R_y + G_x G_y + B_x B_y) \\ \sum_{\mathcal{W}} (R_x R_y + G_x G_y + B_x B_y) & \sum_{\mathcal{W}} (R_y^2 + G_y^2 + B_y^2) \end{pmatrix} \quad (16)$$

$R_x, B_x, G_x, R_y, B_y, G_y$  are the spatial derivatives of the image  $RGB$  in directions  $x$  and  $y$ . After computation of the singular values  $\lambda_1$  et  $\lambda_2$  of this matrix, the point is accepted if  $\min(\lambda_1, \lambda_2) > S_\lambda$ , where  $S_\lambda$  is a threshold which is fixed by the user. In addition, in order to take the singularity of most colour invariants into account (most of them are not defined for unsaturated colours), we improve the detection by weighting each component of the matrix by the saturation value  $S = 1 - \frac{3 \min(R, G, B)}{R+G+B}$  of the pixel. This ponderation reduces the number of points that are selected (30 % on average in the sequences of this article).

### Comparison of the methods

A point is rejected of the tracking process if the convergence residuals ( $\varepsilon_1$  and  $\varepsilon_2$ ) become greater than a threshold (15% according to the initial image, which represents a severe threshold according to the illumination changes provoked). The window size is  $\mathcal{N} = 15$ . In order to evaluate the robustness and accuracy of the methods, we compute :

- the number of points that are correctly tracked by each tracker during the sequence, for each method ( $\varepsilon_1$  or  $\varepsilon_2$ ), and for each colour attribute ( $GL$  refers to the gray level image);

- the convergence residuals of some of the most relevant techniques. The lower the residuals are the more the lighting changes are compensated for. Moreover, when residuals remain low during the whole sequence, it is more probable that the estimated locations of the points are correct.

First, the comparison is achieved on two sequences showing specular highlights. Secondly, lighting changes are caused.

## Specular highlights variations

### Sequence 1

The first sequence (see Fig. 2(a)) represents a painting under glass which is moved by an operator. The camera is motionless. The movement of the object with respect to the lighting (daylight and several fluorescent lights) induces the occurrence of specular highlights. No lighting change is caused.

The number of points which are correctly tracked (on 10 points selected initially) is counted in the table of Fig. 2.(b), with respect to the approach : minimization of  $\epsilon_1$  or  $\epsilon_2$ . By using the first technique ( $\epsilon_1$ ),  $L_2$  norm and  $c_1c_2c_3$  obtain the best robustness results in comparison to the other techniques including  $a_1a_2a_3$  which are theoretically dedicated to specular materials.

Then, the joint use of a photometric model with colour attributes provides some quite satisfying results (minimizing of  $\epsilon_2$ ). Two important points have to be underlined. First of all, the method using  $RGB$  components and the photometric model loses less points than the same approach in luminance images (GL with model), and it loses less points in comparison to the use of colour invariants ( $L_2$  with model for example). Secondly, the joint use of the norm  $L_2$  and the photometric model obtains the same results. It is also interesting to notice that these two methods are more relevant than the use of  $a_1a_2a_3$  when specular highlights changes are concerned.

Fig. 2 (c) compares the convergence residuals obtained with the classical approach  $RGB$ , the use of the photometric model and the joint use of invariant with the model ( $L_2$ +model). At  $50^{th}$  frame, the classical method loses all of the points, whereas the methods involving a photometric model ( $RGB$ +model et  $L_2$  + model) get low residuals during the whole sequence. Finally,  $L_2$ +model compensates for specular highlights more significantly.

### Sequence 2

The second sequence (Fig. 3(a)) represents a hardback box whose surface is smooth and specular. Let us notice that the colours are less saturated compared to the previous sequence. Both camera and lighting are motionless. The intensity of light does not change but some specular highlights appear because of the motion undergone by the object with regard to the spotlights and to the camera.

Initially, 36 points are detected. As it is shown by the number of points that are correctly tracked (table of Fig. 3(b)), the use of the photometric model significantly improves the robustness. Moreover, these results are more convincing with  $RGB$  components in comparison with the use of colour invariants. That result can be explained by the fact that the colours are less saturated in comparison with the first sequence, and colour invariants are less efficient in those conditions. Thus, the use of method  $\epsilon_2$  is clearly justified in that case.

Fig. 3(c) shows the residues obtained with  $RGB$ +model,  $c_1c_2c_3$ +model and  $RGB$ . The latter loses all of the points at the  $25^{th}$  frame.  $L_2$ +model obtains the lowest residuals although the number of points that are correctly tracked is lower than  $RGB$ +model (see table of Fig. 3(c)). Indeed, despite the points detection method, the use of invariants comes up against the occurrence of noise for unsaturated colours during the image sequence.

## Lighting changes

### Sequence 3

The third sequence (Fig. 4(a)) shows several objects of various materials, which are lighted by one fluorescent lighting and one halogen lamp. Only the camera is moved. The scene is composed of specular surfaces, and illumination variations are provoked by the occurrence of shadows that are cast on the objects. Table of Fig. 4(b) registers the number of points that are correctly tracked, on 39 points initially selected. The joint use of invariants with a photometric model, and particularly the method  $L_2$ +model, improves significantly the efficiency of the tracking, since it loses less points than any other approach. In a similar manner as in second sequence, method  $c_1c_2c_3$ +model obtains the lowest convergence residuals, which proves its accuracy. Let us notice that the attributes  $a_1a_2a_3$  ensure a correct robustness. In comparison with the previous experiments, their contribution is more relevant when lighting changes are caused than when only specular highlights are provoked.

### Sequence 4

The image sequence of Fig. 5(a) represents a few objects of different materials under several lightings (daylight, fluorescent, halogen light). 15 points can be tracked during the sequence, the others go out of the field of view of the camera. A lamp is switched off at the  $40^{th}$  image and the fluorescent lamp is switched off at its turn in the  $60^{th}$  frame. Both are switched on at iteration 80. The camera undergoes a rotation motion. The number of points which are correctly tracked attests the robustness of methods which jointly involve colour invariants and photometric model (see table of Fig. 5(b), where  $c_1c_2c_3$ +model and  $L_2$  +model track a larger number of points in comparison with any other technique). Fig. 5(c) and Fig. 5(d) display the residuals as a function of the frame number. Only the most convincing approaches are shown :  $RGB$ +model and  $L_2$  on Fig. 5(c),  $L_2$ +model and  $c_1c_2c_3$ +model on Fig. 5(d). First of all, the residuals of  $RGB$ +model reach lower values than  $L_2$ . Thus, the model is more adapted to the photometric changes provoked, although it only compensates for a local approximation of these changes, unlike colour invariants. Finally,  $L_2$ +model is more relevant, judging by the weak level of its residuals. Let us notice that the residuals obtained by the different approaches are especially high when the lamps are switched off (from frame 60 to frame 80). This remark highlights the weakness of these colour invariants which are not efficient when the saturation of the colours are drastically reduced.

## Computation time

The computation time of the tracking is a crucial criterion for some computer vision applications. Unfortunately that is the main limitation of colour tracking. For a window size 11 the classical approach KLT [9, 13] takes about 3 ms for a point, whereas

the same approach takes 7ms in colour images. To finish, the minimization of (12) takes 15 ms in colour images, and only 5 ms in luminance images. These have been obtained with a processor AMD Athlon, 1,8 GHz, and a RAM of 512 Mb.

## Discussions

A few remarks have to be underlined. First of all, colour invariants defined for specular surfaces have not proved to be really efficient in the context of points tracking. In the one hand, they are noisy when colours are not saturated enough ( $R \simeq G \simeq B$ ). In the other hand, they are likely to reduce the discriminative power between colours.

In each sequence, the tracking methods using colour invariants, in particular the  $L_2$  norm and  $c_1c_2c_3$  attributes, is more robust than the use of the only luminance or the colour since less points are lost in general. Broadly speaking, the joint use of a photometric model and colour improves the tracking results in a more efficient way. It is even more efficient to jointly use  $L_2$  ou  $c_1c_2c_3$ , which are only valid for inhomogeneous and dull dielectric surfaces, with a photometric model that makes up for specular variations. However, when colours are not saturated enough (as in sequence 2) and when specular highlights are caused, we obtain better results by using *RGB* components with the photometric model.

To improve the tracking, the detection of points should be dedicated to the tracking method which is carried out. However, in order to compare the tracking techniques, we have selected the same points for each method.

## Conclusion

In this article, we have proposed three methods to improve points tracking in colour images : by computation of a local photometric model, by a global compensation of illumination changes (use of colour invariants) and by the joint use of colour invariants with a photometric model. Even if the invariants improve the tracking results in comparison to the classical approach in *RGB* space, especially when lighting changes are produced, the joint method has proved to be the most efficient whatever the illumination changes are : specular highlights changes and lighting variations. Unlike the use of invariants defined for specular objects, the latter can compensate for illumination changes even if a white balance is not carried out.

In addition, the experiments have highlighted the fact that the main drawback of colour invariants is their inefficiency when colours are not saturated. Thus, our future works will deal with the detection of points and the fusion of luminance information and colour invariants to achieve tracking whatever the saturation of the colours.

## Acknowledgments

The authors thank the Cemagref of Rennes, the OFIVAL ( Office national interprofessionnel des viandes, de l'élevage et de l'aviculture) and the county council of Poitou-Charentes for the funding of the global project including these researches.

## Références

[1] F.X. Espiau, E. Malis, and P. Rives. Robust features tracking for robotic applications : towards 2 1/2 D visual servoing with natural images. In *IEEE Int. Conf. on Robotics and Automation*, Washington, USA, 2002.

[2] T. Gevers and A.W.M. Smeulders. Color based object recognition. *Pattern Recognition*, 32 :453–464, 1999.

[3] V. Gouet, P. Montesinos, R. Deriche, and D. Pelé. Evaluation de détecteurs de points d'intérêt pour la couleur. In *Reconnaissance de Formes et Intelligence Artificielle*, pages 257–266, Paris, 2000.

[4] M. Gouiffès, C. Collewet, C. Fernandez-Maloigne, and A. Trémeau. Feature points tracking : robustness to specular highlights and lighting changes. In *European Conference on Computer Vision*, 2006.

[5] P. Gros. Color illumination models for image matching and indexing. In *International Conference on Pattern Recognition*, Barcelona, Spain, September 2000.

[6] C.G. Harris and M. Stephens. A combined corner and edge detector. In *4th Alvey Vision Conference*, pages 147–151, 1988.

[7] B. Heigl, D. Paulus, and H. Niemann. Tracking points in sequences of color images. In *German-Russian workshop Pattern Recognition and Image Understanding*, pages 70–77, Herrsching, Germany, 1999.

[8] H. Jin, S. Soatto, and P. Favaro. Real-time feature tracking and outlier rejection with changes in illumination. In *IEEE Int. Conf. on Computer Vision*, pages 684–689, Vancouver, Canada, 2001.

[9] B.D. Lucas and T. Kanade. An iterative image registration technique. In *IJCAI'81*, pages 674–679, Vancouver, British Columbia, 1981.

[10] S. Negahdaripour. Revised definition of optical flow : integration of radiometric and geometric cues for dynamic scene analysis. *IEEE Transactions on Pattern Analysis and Machine Intelligence*, 20(9) :961 – 979, 1998.

[11] B-T Phong. Illumination for computer generated images. *Communications of the ACM*, 18(6) :311–317, 1975.

[12] S.A. Shafer. Using color to separate reflection components. *Color Research and Applications*, 10(4) :210–218, 1985.

[13] C. Tomasi and T. Kanade. Detection and tracking of point features. Technical report CMU-CS-91-132, Carnegie Mellon University, 1991.

[14] T. Tommasini, A. Fusiello, E. Trucco, and V. Roberto. Improving feature tracking with robust statistics. *Pattern Analysis & Applications*, 2 :312–320, 1999.

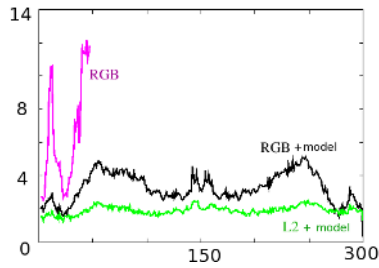
[15] K.E. Torrance and E.M. Sparrow. Theory for off-specular reflection from roughened surfaces. *Journal of the Optical Society of America*, 57(9), 1967.



(a)

Attributes	$\varepsilon_1$ (eq. (11)) without model	$\varepsilon_2$ (eq. (12)) with model
GL	0	6
RGB	0	7
$L_1$	0	3
$L_2$	3	7
$c_1c_2c_3$	3	4
$a_1a_2a_3$	0	-

(b)



(c)

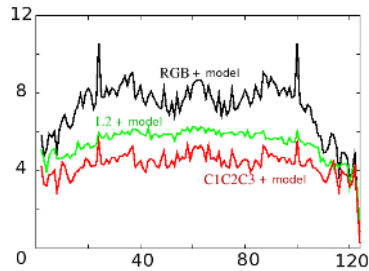
**Fig. 2.** Sequence 1. (a) : two images of the sequence. (b) : number of points which are correctly tracked (on 10 points initially selected). (c) and (d) : convergence residuals obtained for  $\mathcal{N} = 15$ .



(a)

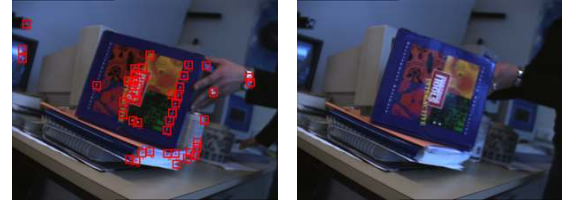
Attributes	$\varepsilon_1$ (eq. (11)) without model	$\varepsilon_2$ (eq. (12)) with model
GL	0	11
RGB	3	22
$L_1$	20	21
$L_2$	30	33
$c_1c_2c_3$	20	28
$a_1a_2a_3$	29	-

(b)



(c)

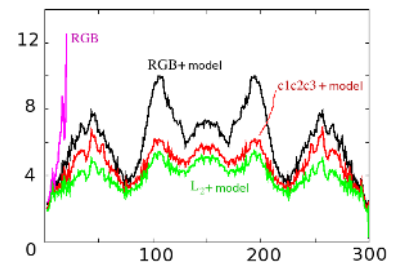
**Fig. 4.** Sequence 3. (a) : two images of the sequence. (b) : number of points which are correctly tracked (on 39 points initially selected). (c) and (d) : convergence residuals obtained for  $\mathcal{N} = 15$ .



(a)

Attributes	$\varepsilon_1$ (eq. (11)) without model	$\varepsilon_2$ (eq. (12)) with model
GL	0	9
RGB	0	25
$L_1$	2	3
$L_2$	5	18
$c_1c_2c_3$	3	20
$a_1a_2a_3$	0	-

(b)



(c)

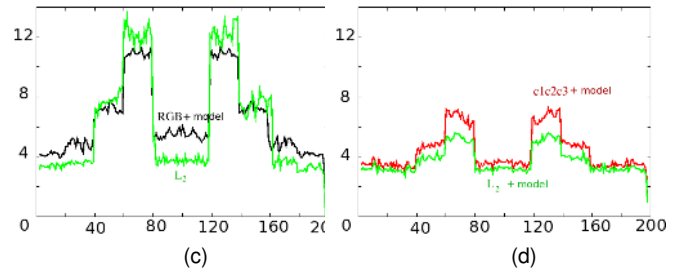
**Fig. 3.** Sequence 2. (a) : two images of the sequence. (b) : number of points which are correctly tracked (on 36 points initially selected). (c) and (d) : convergence residuals obtained for  $\mathcal{N} = 15$ .



(a)

Attributes	$\varepsilon_1$ (eq. (11)) without model	$\varepsilon_2$ (eq. (12)) with model
GL	0	0
RGB	0	4
$L_1$	0	3
$L_2$	4	8
$c_1c_2c_3$	3	8
$a_1a_2a_3$	3	-

(b)



(c)

(d)

**Fig. 5.** Sequence 4 (a) : two images of the sequence. (b) : number of points which are correctly tracked (on 15 points initially selected). (c) and (d) : convergence residuals obtained with  $\mathcal{N} = 15$ .